Synthesis and characterization of ceria-supported catalysts for carbondioxide transformation to diethyl carbonate

Ewelina Leino, Narendra Kumar, Päivi Mäki-Arvela, Anne-Riikka Rautio, Johnny Dahl, Jorma Roine, Jyri-Pekka Mikkola

Abstract

The support materials Al_2O_3, SiO_2 and TiO_2 were modified with 16 wt% CeO_2, using two different preparation methods evaporation-impregnation and precipitation-deposition. The synthesized 16 wt% CeO_2-Al_2O_3, 16 wt% CeO_2-SiO_2 and 16 wt% CeO_2-TiO_2 materials were characterized by means of X-ray powder diffraction for the phase purity, scanning electron microscopy for the morphology, nitrogen physisorption to determine the specific surface area and X-ray photo electron spectroscopy for the oxidation state of the Ce in the TiO_2, Al_2O_3 and SiO_2 matrices. Transmission electron microscopy was used to study the particle size of CeO_2 whereas CO_2-temperature programmed desorption (TPD) was used to determine the basicity of ceria-modified TiO_2, Al_2O_3 and SiO_2 catalysts. Furthermore, the catalytic performance of the as prepared CeO_2-modified catalysts were compared in the synthesis of diethyl carbonate starting from ethanol and CO_2 using butylene oxide as the dehydrating agent. The physico-chemical characterization results were correlated with the catalytic activity results and discussed in detail.

1. Introduction

Over the past few decades, rare-earth oxides have gained substantial attention and have been widely investigated as structural and electronic promoters to improve the activity, selectivity and thermal stability of catalysts. Undoubtedly, cerium oxide (CeO_2) is the most significant one of rare-earth element oxides in the industrial catalysis owning to its unique structural, redox and acid-base properties [1]. Due to the high oxygen storage capacity arising from the ability to be easily and reversibly reduced, ceria has become a key component in the three way catalysts (TWC) [1], [2]. Simultaneously, ceria provides key features that are utilized in the most efficient route to reduce pollutants released from automotive exhaust gases. Moreover, cerium oxide finds use in a wide range of other applications and is applied as UV absorbents and filters [3], glass polishing material [4], oxygen ion conductor in solid oxide fuel cells (SOFCs) [5], catalytic wet oxidation catalyst [6], NO removal catalyst [7] as well as being an important catalyst support and promoter [8], [9], [10].

Frequently, supported-catalysts are given preference over the individual components due to their combined and comprehensive properties which enable to overcome the shortcomings of the single phase materials. Since cerium oxide exhibits rather low specific surface area, its dispersion on the high specific surface area supports such as SiO_2, Al_2O_3 and/or TiO_2 could represent a suitable way of enhancing the amount of the active sites available for the reaction and, at the same time, stabilize the structural/textural and acid-base properties of CeO_2. Numerous studies on ceria dispersed on SiO_2 and Al_2O_3 have been conducted whereby the thermal durability of alumina and silica played an important role in case of processes performed at high temperatures. Examples thereof include gas purification, high temperature hydrogen separation as well as catalytic membrane reactors [11], [12], [13], [14], [15]. In turn, titanium oxide finds broad application in heterogeneous catalysis as a catalyst and catalyst support [16]. Besides anatase phase, TiO_2 can also be

present as rutile and brookite phases, depending on the synthesis method and calcination temperature. It was demonstrated that introduction of refractory modifiers such as cerium oxide improves resistance to thermal loss and stabilize the active phase of TiO_2 in CuO/Ce-TiO_2 catalysts for the oxidation of CO, ethanol, ethyl acetate [17] and in NO + CO reduction [18].

This study, however, was focused on in-house synthesis and characterization of ceria-based catalysts supported on silica, alumina and titanium oxide applying different synthesis methods and varying ceria loading and calcination temperature. The catalytic activities of prepared materials were compared in the reaction of carbon dioxide transformation to diethyl carbonate (DEC).

DEC is an important homologue in the family of dialkylcarbonates possessing eco-friendly features such biodegradability to ethanol and carbon dioxide. Moreover, the fact that it can be prepared from bioethanol gives a "bio-derived" label to DEC and all the processes in which it is applied. DEC is used in a variety of applications such as a raw material upon manufacturing of polycarbonates, an intermediate for various pharmaceuticals, an electrolyte in lithium ion batteries and as an alternative to ethyl halides and phosgene in ethylation and carbonylation processes [19], [20]. Furthermore, DEC is also considered as a promising replacement for methyl-tert-butyl ester (MTBE) as an attractive oxygen-containing fuel additive due to its high oxygen content (40.6%). Conventional synthesis method of DEC involves the use of extremely poisonous phosgene [21] and, therefore, considerable effort has been devoted to the development of alternative technologies such as transesterification of methanol [22], oxidative carbonylation of ethanol [23], carbonylation of ethyl nitrite [24], reaction of ethanol with urea [25] and decarbonylation of diethyl oxalate [26]. Nevertheless, the practical application of these non-phosgene routes is still restricted due to several disadvantages such as the toxicity of carbon monoxide and ethyl nitrite, deactivation of the catalysts and low product yields.

Recently, global warming and successive climate change have gained much attention gathering scientists and engineers from the academia and industry on seeking for new ideas of mitigation of greenhouse gases from the Earth's atmosphere. Carbon dioxide has been considered to be the most prominent greenhouse gas. Therefore, it is not surprising that transformation of CO_2 to other value-added chemicals is today a subject of intensive studies from the standpoint of the environment protection. New technologies such as diethyl carbonate synthesis via a direct route starting from inexpensive and non-toxic ethanol and CO_2 is certainly an attractive approach (Eq. (1)). It should be, however, emphasized that during the last years dimethyl carbonate (DMC) and not diethyl carbonate, has been the main subject of studies in the industry and academia. Therefore, this work has been entirely devoted to the synthesis of diethyl carbonate over in-house made supported ceria catalysts.

$$C_2H_5OH + CO_2 \rightleftharpoons (C_2H_5O)_2CO + H_2O \quad (1)$$

Thermodynamic calculations of direct synthesis of DEC revealed that the reaction is exothermic ($\Delta_rH\Theta_{298K}$ = −16.60 kJ/mol) and does not occur spontaneously under normal conditions ($\Delta_rG\Theta_{298K}$ = + 35.85 kJ/mol > 0) [27]. Moreover, the carbonate synthesis is accompanied with water release (Eq. (1)) which easily shifts the reaction equilibrium towards the reactants. Thus, in situ dehydration in direct carboxylation of ethanol could be a powerful methodology to reach an enhanced production of the desired product. The yield of DEC approaching 42% (based on CO2) was achieved after 24 h reaction time at 423 K and 0.2 MPa of CO_2 pressure applying acetonitrile as the chemical water trap [28]. In addition, a flow reactor was coupled with a pervaporation membrane in order to decrease water content and increase the conversion of ethanol from 0.9 up to 2.3%, resulting in relatively pure DEC (>90%) [29]. Our previous studies, in turn, demonstrated a 9-fold enhancement in the yield of DEC using butylene oxide as the dehydrating agent, in comparison to the synthetic method without any water removal over commercial ceria [27].

Up to date cerium oxide is one of the most studied catalyst in the synthesis of dimethyl and diethyl carbonate [30], [31], [32] and it has been identified that basic sites are the active sites in the synthesis of DEC.,Also, ceria-zirconia ($Ce_xZr_{1-x}O_2$) mixed oxides with tunable Ce/Zr ratios were investigated and it was demonstrated that $Ce_xZr_{1-x}O_2$ (x = 1) exhibited the highest activity towards DEC followed by $Ce_xZr_{1-x}O_2$ (x = 0.7). This could be attributed to the strong dependence of catalytic properties of $Ce_xZr_{1-x}O_2$ on the crystal structure and the acid-base sites on the surface with varied Ce/Zr ratios. [33]. Additionally, a highly efficient approach was demonstrated in one-pot synthesis of DEC starting from ethanol, ethylene oxide and CO_2 over KI-based binary catalytic system yielding 63.6% of DEC at 443 K and 3 MPa of CO_2 initial pressure [34]. Moreover, it was shown that 3–10 wt% loading of ceria on alumina with respect to pure ceria prolongs the life-time of the catalyst and improves both the catalytic performance as well as the selectivity towards dimethyl carbonate [8].

Nevertheless, none of the currently available reports in the open literature discuss the one-pot synthesis of DEC starting from CO_2, ethanol and butylene oxide over ceria-supported onto SiO_2, Al_2O_3 and TiO_2 materials. Hence, in this work, the influence of synthesis method of SiO_2, Al_2O_3 and TiO_2 supported ceria catalysts, ceria loading and calcination temperature on the physico-chemical properties of the resulting catalyst was for the first time correlated to the catalytic activity of these materials in DEC synthesis. Since solid base catalysts are preferred over acid catalysts in the synthesis of this linear carbonate particular attention has been paid to the basicity of prepared composites.

2. Experimental

2.1. Catalyst preparation

Catalysts were prepared using SiO_2 (Merck), Al_2O_3 (UOP Versal VGL-25) and TiO_2 (Alfa Aesar) as supports. The support materials were ball-milled and sieved to obtain a particle size smaller than 63 μm. An aqueous solution of cerium (III) nitrate hexahydrate (Sigma Aldrich 99.0%) was used as a ceria precursor. The samples were synthesized applying evaporation-impregnation and deposition-precipitation methods.

In line with the evaporation-impregnation method, 10 g of the metal oxide support materials were added to the solution of the desired amount of cerium (III) nitrate hexahydrate in 250 ml of distilled water. The solution was stirred in a rotary-evaporator for 24 h at 60 °C and, subsequently, water was evaporated under vacuum. The catalyst was dried overnight at 100 °C and calcined at the pre-determined temperature for 3 h.

Upon preparation of the supported CeO_2 catalysts via deposition-precipitation method, 1 M aqueous solution of cerium (III) nitrate hexahydrate was prepared and pH of the solution was adjusted to 11 by the addition of ammonium hydroxide (NH_4OH) (Sigma-Aldrich, ACS reagent 28.0–30.0%). The support material was added and the suspension was kept under continuous stirring for 50 h, at room temperature. Afterwards, the suspension was filtrated, washed with water, dried overnight at 100 °C and calcined at the specified temperature for 3 h.

2.2. Catalyst characterization

The structural properties of the support materials and ceria-supported catalysts were investigated by Philips X'Pert Pro MPD X-ray powder diffractometer. The diffractometer was operated in Bragg-Brentano diffraction mode and the monochromatized Cu-Kα radiation was generated with a voltage of 40 kV and a current of 50 mA. The measured 2θ angle range was 3.0°–75.0°, with a step size of 0.04° and measurement time of 2.0 s per step. The average crystal size was estimated for each crystalline phase from the measured X-ray diffractogram by the Rietveld refinement method, using Maud software (v. 2.33) [35]. A Si standard powder sample was measured to determine the instrumental broadening function.

Elemental content of the samples was analyzed by FESEM-EDX (Zeiss Ultra plus equipped with an energy dispersive X-ray spectroscopy analyzer).

The specific surface area of the catalyst was determined by measuring the nitrogen adsorption-desorption isotherms (Sorptomatic 1900, Carlo Erba) at 77 K. Before each measurement, the samples were outgassed for 3 h at 423 K to a residual pressure below 0.01 Pa. The total surface area was calculated according to the B.E.T. equation.

The basicity of the obtained samples was determined by means of temperature programmed desorption (TPD) of CO_2 using Micromeritics Instrument (AutoChem 2010). In short, 0.25 g of catalyst was placed in a quartz made U shaped tube. The catalyst was first dried under helium flow, followed by adsorption of CO_2, flushing of physisorbed CO_2 and temperature programmed desorption up to the temperature of 600 °C.

X-ray photoelectron spectroscopy (XPS) was used to determine the oxidation state of Ce. The x-ray photoelectron spectra were measured using a Perkin-Elmer PHI5400 spectrometer with a monochromatized Al Kα source. The core-level emissions investigated were Ce 3d, O 1s, Si 2p, Al 2p and Ti 2p. The eV/step was 0.1 and the pass energy was 17.90 eV. The samples accumulated charge and the use of a charge neutralizer electron gun was necessary. Each spectrum was fitted with the Voigt functions.

2.3. Catalytic tests

All experiments were carried out in a laboratory scale stainless steel autoclave (Parr Inc) with an inner volume of 300 ml equipped with a stirrer and an electric heater. In a standard procedure, 1 g of catalyst, 314 mmol of ethanol (Etax, Aa, 99.5%) and 19 mmol of dehydrating agent 1,2-epoxybutane (Fluka, ≥99.0%) were charged into the autoclave and the reactor was purged and pressurized to 4.5 MPa with CO_2 (AGA 99.99%), at room temperature. The reactor was heated and mechanically stirred constantly at the desired temperature during the reaction. After the reaction, the reactor was cooled to about 278 K and depressurized.

2.4. Product analysis

The products in the liquid phase were analyzed by means of gas chromatography (Agilent Technologies, 6890N) using capillary columns (HP-Wax 30 m × 250 µm × 0.25 µm and DB-Petro 100 m × 250 µm × 0.5 µm). The reproducibility of the results was confirmed by analyzing each sample twice. The peaks in the chromatogram were identified with the following reference substances: diethyl carbonate (Sigma, 99%), ethanol (Etax, Aa, 99.5%), 1,2-epoxybutane (Fluka, ≥ 99.0%), 1,2-butanediol (Fluka, 98%). The products were also indentified by means of GC–MS (Agilent Technologies, 6890N) using capillary column (DB-Petro 50 m x 200 µm x 0.5 µm).

3. Results and discussion

3.1. Influence of the synthesis method on the physico-chemical properties of supported ceria materials

16 wt% ceria was deposited onto SiO_2, Al_2O_3 and TiO_2 supports applying evaporation-impregnation (evimp.) and deposition-precipitation (dp.) methods, respectively. All materials underwent typical calcination at 600°C for 3 h in air. The influence of the synthesis method on the morphology, surface area and basicity of the prepared materials was studied. X-ray powder diffraction (XRD) analysis results conducted on the catalysts synthesized via evaporation-impregnation are shown in Fig. 1. Similar XRD patterns were collected for samples prepared by deposition-precipitation. The XRD results clearly demonstrated, for all materials, the presence of well-crystallized CeO_2 with two characteristic XRD peaks for the cubic fluorite phase in CeO_2 at 2θ = 28.6° and 33.1° corresponding to (111) and (200) peaks for CeO_2, in accordance to the literature [36], [37], [38], [39]. In addition, 2θ equal to 47.5°, 56.4°, 59.1° and 69.5° correspond to CeO_2 (220), (311), (222)

and (400), respectively. Moreover, all XRD pictures contain Cu(111) and Cu(200) peaks originated from 2θ 43.3° and 50.5°. In case of 16 wt% CeO_2-SiO_2 and 16 wt% CeO_2-Al_2O_3, the CeO_2 particle sizes were quite close to each other, in spite of the fact that the former material possessed a larger specific surface area (Table 1). In case of 16 wt% CeO_2-TiO_2 material, the cerium oxide particle size was quite small compared to its specific surface area.

A broad peak of pure silica at around 2θ = 23° confirms an amorphous character of SiO_2 support (Fig. 1a). It can be observed that silica peak intensity of 16 wt% CeO_2-SiO_2 is much weaker than that of the pure SiO_2 powder. In agreement to the literature, the likely reason for this is that silica particles may be well coated with ceria and the outer CeO_2 particles may prevent the diffraction of inner SiO_2 at least to some degree [40]. Furthermore, three diffraction peaks characteristic for crystalline γ-Al_2O_3 located at 2θ = 37.7°, 46.0° and 66.9° corresponding to (211/103), (220/004) and (224) peaks, can be observed for the pristine Al_2O_3 material (Fig. 1b) [39]. No further peaks in addition to ceria and γ-Al_2O_3 corresponding to any other possible phase could be observed in case of 16 wt% CeO_2-Al_2O_3, thus indicating good stabilization of alumina by ceria [41], [42].The XRD patterns of pure titanium oxide and 16 wt% CeO_2-TiO_2 (Fig. 1c) confirmed, in both samples, the presence of anatase phase of TiO_2 with characteristic reflections at 2θ = 25.2°, 38.6°, 48.1° and 55.1° corresponding to (101), (112), (200) and (211) peaks, respectively [38], [39], [43]. The conventional unit cell in the anatase phase contains four TiO_2 units in which each oxygen atom is coordinated to three Ti atoms lying all in the same plane [44].It is noteworthy that although CeO_2-TiO_2 was calcined at 600 °C, no rutile was detected which is contradictory to literature data reporting that anatase phase should change to rutile between 500 °C to 600 °C [45]. A plausible explanation for such behaviour of the 16 wt% CeO_2-TiO_2 catalyst may be the presence of large amounts of CeO_2 in this composite material that stabilized the anatase phase.

Scanning and tranmission electron micrographs of ceria-supported materials prepared by evaporation-impregnation and deposition-precipitation method are presented in Fig. 2. Morphological differences between 16 wt% CeO_2-SiO_2 samples can be observed. The one synthesized applying evaporation-impregnation technique clearly shows uniform morphology and relatively well-dispersed ceria over silica (Fig. 2a), whereas 16 wt% CeO_2-SiO_2 composite prepared via deposition-precipitation exhibits aggregation of ceria particles in variable size aggregates and overall non-uniform dispersion within the silica matrix. On the other hand, both samples of alumina supported ceria displayed rather similar overall structures (Fig. 2b) in which interconnected rod-like particles of γ-Al_2O_3 make up sort of the three dimensional porous structure. Micrographs of ceria deposited on titanium oxide materials, in turn, show in both cases fully crystalline anatase grains consisting of a mass of rather small crystals.

X-ray photoelectron spectroscopy analysis was conducted in order to obtain additional information on structural properties of cerium oxide deposited onto metal oxide support materials. The Ce 3d spectra collected for ceria-supported samples prepared applying different synthesis methods are depicted in Fig. 3. The results confirmed in case of all analyzed composites the presence and predominance of tetravalent Ce ions (Ce^{4+}). More than 70% of the total cerium surface ions resided in the oxidation state Ce^{4+}. However, the co-existence of trivalent Ce ions (Ce^{3+}) could also be distinguished. The labels shown in Fig. 3a follow the convention introduced by Burroughs et al. where V and U indicate the spin-orbit coupling 3 $d_{5/2}$ and 3 $d_{3/2}$, respectively [46]. The Ce^{3+} and Ce^{4+} can be differentiated with distinct line shapes corresponding to the particular final states: Ce (3 +) = V^0 + V' + U^0 + U' and Ce (4 +) = V + V" + V"'' + U + U" + U"'. The satellite peak U"' associated to the Ce $3d_{3/2}$ is a characteristic feature hinting to the presence of tetravalent Ce ions in ceria compounds which is in good agreement with other literature reports [47], [48]. Its absence in the Ce (3 +) spectrum is characteristic when no $4f^0$ state is present in these compounds. The highest binding energy peaks of tetravalent Ce ions, U"' and V"' and located at about 915 eV and 895 eV, respectively, are the result of a Ce $3d^9$ $4f^0$ O 2p6 final state. The peaks with the lowest binding energy U, V, U", V", located at about 898 eV, 878 eV, 904 eV and 885 eV, respectively, can be ascribed to Ce $3d^9 4f^2$ O $2p^4$ and Ce $3d^9 4^{f1}$ O $2p^5$ final states.

In case of Ce^{3+} ions, in turn, the highest binding energy peaks, U' and V', located at about 903 eV and 885 eV, respectively, are the result of a Ce $3d^9 4f^1$ O $2p^6$ final state. The lowest binding energy states U0 and V0, located at about 899 eV and 881 eV, respectively, are arising from Ce $3d^9 4f^2$ O $2p^5$.

The binding energy of the Al 2p photoelectron peak (Fig. 4a), located at about 75 eV, is in good agreement with literature reports [49], [50]. The spectrum is relatively broad indicating that alumina is not easily accessible at the surface due to the presence of ceria over layer. Similarly, Ti 2p XPS spectrum (Fig. 4b) with doublet of TiO_2-anatase phase, at approximately 459 eV and 464 eV, and with the relative intensity (2:1) is consistent with the literature reports [51], [52].

It has been previously reported that solid base catalysts are preferred over acid catalysts in the synthesis of diethyl carbonate, owning to the high yields of linear carbonate produced and reduction of the side-reactions [53], [54]. Therefore, in this work, special consideration was paid on the basicity of the prepared supported materials. The amount and strength of the basic sites present on the surface of ceria modified catalysts was determined by means of temperature programme desorption (TPD) using carbon dioxide as the probe molecule. CO_2-TPD profiles of synthesized materials (Fig. 5) consist of three strength distributions namely weak, medium and strong which for ceria-containing catalysts have been identified as OH groups, M–O site pairs with accessible cations and strongly basic O_2− surface anions, respectively. Moreover, certain differences in the basic properties of the unmodified support materials can be observed from CO_2-TPD profiles. Pure SiO_2 and γ-Al_2O_3 exhibit distinct CO_2 desorption peaks of weak and strong character whereas pristine TiO_2 shows primarily presence of moderate basic sites on its surface. However, modification of TiO_2 with ceria expands CO_2 adsorption capacity leading to the enhancement of weak and strong type of basic sites.

The amount of basic sites was estimated from the peak area under the TPD curves for the temperature range of 320K − 500K, 500K − 750K and >750K, respectively, and is summarized in Table 1, together with the specific surface area of the samples. Pure γ-Al_2O_3 displays greater basicity in comparison to silica and titania supports. It can be also seen that, in all cases, deposition of ceria upon the metal oxide supports resulted in an increase in the total basicity of the modified materials. This is also in agreement with our previous findings on mesoporous MCM-41 loaded with CeO_2 [55]. Nevertheless, variations in the synthesis method during the preparation of ceria-supported catalysts did not give rise to any explicit impact in terms of the basicity of the catalysts. Furthermore, SiO_2 possessed the highest specific surface area among all support materials (Table 1) followed by γ-Al_2O_3 which upon modification with CeO_2 gave materials with decreased surface area. Analogously, only a rather minor decrease in the specific surface areas were observed when loading 12 wt% CeO_2 on alumina and 10 wt% CeO_2 on silica, respectively [56], [57]. Titanium oxide exhibited the lowest specific surface area which in contrast to silica and alumina diminished rigorously upon deposition of CeO_2. This was observed in case of both the evaporation-impregnation and deposition-precipitation synthesis method. A similar phenomenon has been already observed and it was shown that TiO_2 nanoparticles tend to agglomerate intensively during the calcination at high temperatures leading to a substantial decrease in the specific surface area. This is also likely the reason in case of 16 wt% CeO_2-TiO_2 materials since they underwent calcination at 600 °C during the material preparation procedure [58]. The reason for the enormous decrease in surface area of 16 wt% CeO_2-TiO_2 is attributed to the increase in the crystallite size of TiO_2 (33.6 nm), while in case of the pristine TiO_2 the crystallite size was 19.4 nm determined by XRD.

3.2. Influence of the ceria loading and calcination temperature on the physico-chemical properties of ceria-supported on SiO_2 materials

A series of CeO_2-SiO_2 catalysts with varying ceria loadings were prepared via evaporation-impregnation method in order to correlate the ceria loading with their physico-chemical properties.

First, silica support was modified with 8 and 32 wt% of ceria, respectively. The XRD patterns of the samples are illustrated in Fig. 6. The intensity of the amorphous silica peak decreases with the increase of ceria loading suggesting that the structure of the support is strongly influenced by ceria addition.

Moreover, the characteristic peaks confirming CeO_2 crystallized in a face-centered cubic structure can be observed for all CeO_2-SiO_2 powders. The diffraction intensities of four ceria peaks of 16 and 32 wt% CeO-SiO_2 are similar indicating comparable crystallinity as confirmed by the average crystal sizes of the materials (Table 2). Additionally, the reason for higher diffraction intensities of 16 and 32 wt% CeO-SiO_2 powders with respect to 8 wt% counterpart was, undoubtedly, the increased ceria loading. As expected, the specific surface area of the pristine support material was the highest (389 m^2/g) and it gradually decreased due to ceria particles depositing and agglomerating on its surface (Table 2). The 32 wt% CeO_2-SiO_2 catalyst exhibited the lowest specific surface area, most probably because of high ceria loading causing certain blocking of the pores of the silica support. Furthermore, an increase in the amount of CeO_2 dispersed on silica first resulted in an enhancement of the total basicity of the material, followed by a slight decline upon reaching 32 wt% ceria loading. Similar phenomenon has also been reported for 5 wt% nickel catalysts supported on binary CeO_2-SiO_2 with different ceria loadings where total CO_2 uptake decreased from 750 µmol/g to 484 µmol/g with the enlargement of CeO_2 amount from 18 to 30 wt% [59].

Calcination exposes the as-prepared catalyst precursors to high temperatures upon final stages of the formation of metal oxide catalysts. The primary aim of the calcination process is to thermally decompose non-oxide precursors, remove unwanted ligands and leave behind an impurity-free surface. It is well-known that the thermal energy of calcination influences the crystalline phases, crystal size and surface properties of the material. The influence of the calcination temperature on the properties was examined in case of the 16 wt% CeO_2-SiO_2 catalyst prepared via evaporation-impregnation method. The powder was calcined at three different temperatures, 400 °C, 600 °C and 800 °C, respectively, for 3 h in air. In agreement with previous literature reports, considerable variations in the specific surface area of ceria-silica materials could be observed depending on the calcination temperature (Table 3) [60], [61].

As expected, ceria-silica calcined at 400 °C exhibited the highest specific surface area among this series of catalysts which subsequently declined for samples calcined at 600 °C and 800 °C, respectively. High calcination temperatures induced crystal growth that subsequently lead to a decrease in the specific surface area of the ceria-silica samples. To the best of our knowledge, the influence of calcination temperature on the basicity of ceria supported on silica material has not been specifically reported in open literature. A substantial decrease in the amount of basic sites of CeO_2-SiO_2–800 °C, with respect to the ones calcined at lower calcination temperatures, could be observed, assuredly caused by the decline in the specific surface area of the sample treated at 800 °C.

3.3. Evaluation of the catalytic properties of CeO2 modified TiO2, Al2O3 and SiO2 catalysts in the one-pot synthesis of diethyl carbonate starting from CO2, ethanol and butylene oxide

In this contribution, for the first time, ceria supported on SiO_2, Al_2O_3 and TiO_2 were demonstrated as catalysts in diethyl carbonate synthesis starting from CO_2, ethanol and butylene oxide. Besides, an effort was made to investigate the influence of the synthesis method, ceria loading and calcination temperature on the catalytic activity of the prepared materials.

The highest yield of diethyl carbonate was obtained over the CeO_2-SiO_2 catalyst synthesized by evaporation impregnation method (Fig. 7) what undoubtedly can be attributed to the specific surface area (325 m^2/g) of this catalyst being the highest among all prepared materials (Table 1). Interestingly, CeO_2-Al_2O_3 catalysts that exhibited the highest amount of total basic sites on their surface resulted in lower amounts of DEC produced compared to SiO_2 supported catalysts. The reason for this might be the lower specific surface area of CeO_2-Al_2O_3.

Moreover, 16 wt% CeO_2-SiO_2 prepared via the evaporation impregnation method gave rise to a higher yield of DEC than in case of the precipitation deposition method. This clearly indicates that the synthesis method affected the catalytic properties of silica-supported materials. The lowest yield of DEC among all studied ceria-supported catalysts was observed over CeO_2-TiO_2 catalysts. Obviously, the reason was the low specific surface area of CeO_2-TiO_2 catalysts.

Moreover, the influence of the amount of CeO_2 loading on the yield of diethyl carbonate was studied by synthesizing CeO2 modified with 8 wt%, 16 wt% and 32 wt% CeO_2-SiO_2 catalysts (Fig. 8a). It was observed that the highest ceria loading 32 wt% gave rise to the lowest amount of DEC what may be attributed to the low specific surface area of 32 wt% CeO_2-SiO_2 catalyst and low amount of basic sites present (Table 2).

The average crystallite size of the CeO_2 was also influenced by the loading of CeO_2. The 16 wt% CeO_2-SiO_2 catalyst exhibited the highest activity towards DEC formation and also possessed the highest average crystal size. This indicates that the size of crystal might have an effect on the amount of DEC produced in one-pot synthesis starting from ethanol and CO_2 using butylene oxide as dehydrating agent.

Furthermore, the influence of calcination temperature on the yield of diethyl carbonate was studied. The 16 wt% CeO_2-SiO_2 catalyst was calcined at 400, 600 and 800 °C, respectively (Fig. 8b). As expected, the specific surface area of the 16 wt% CeO_2-SiO_2 catalyst decreased with the increase of the calcination temperature (Table 3). The lowest surface area (192 m^2/g) was measured in case of 16 wt% CeO_2-SiO_2 catalyst calcined at the highest temperature 800 °C. On the contrary, the catalyst calcined at 400 °C exhibited the highest specific surface area (340 m^2/g). Synthesis of DEC carried out over 16 wt% CeO_2-SiO_2 catalyst calcined at 600 °C resulted in the highest amount of DEC formed due to high amount of basic sites on its surface. Consequently, 16 wt% CeO_2-SiO_2 catalyst calcined at 800 °C gave rise to low yields of DEC which can be explained by the low total amount of basic sites (0.4 mmol/g).

4. Conclusions

Ceria supported on Al_2O_3, SiO_2 and TiO_2 were synthesized using evaporation-impregnation and deposition-precipitation methods. The physico-chemical characterization of the prepared catalysts revealed the influence of ceria loading, calcination temperature and preparation technique on the basicity, surface area and state of CeO_2 supported on Al_2O_3, SiO_2 and TiO_2, respectively. Modification of pristine SiO_2 with 16 wt% CeO_2 using evaporation-impregnation and deposition-precipitation resulted in a lower specific surface area and an increase in the total basicity. SiO_2 modified with different ceria loadings (8 wt%, 16 wt% and 32 wt%) resulted in materials with lower specific surface area with increasing loading of CeO_2. It was also observed that an increase in the calcination temperature for 16 wt% CeO_2-SiO_2 resulted in a lower specific surface area of the material. The largest amount of total basic sites (2.9 mmol/g) was observed in case of 16 wt% CeO_2-SiO_2 calcined at 600 °C. The number of total basic sites, however, decreased (0.4 mmol/g) with an increase in the calcination temperature in case of 16 wt% CeO_2-SiO_2 calcined at 800 °C. The method of preparation was observed to influence the yield of diethyl carbonate obtained. The highest activity towards DEC formation was observed over 16 wt% CeO_2-SiO_2 prepared using the evaporation-impregnation method.

Acknowledgements

Dr. Ewelina Leino thanks the Åbo Akademi University Rectors' scholarship. Academy of Finland is acknowledged for funding the initial stages of the research. In Sweden, also the Kempe Foundations, Wallenberg Wood Science Center and Bio4Energy programme are acknowledged. Further, the Swedish Research Council (Vetenskapsrådet) is acknowledged. This work is a part of the activities of the Johan Gadolin Process Chemistry Centre.

References

[1] E. Finocchio, M. Daturi, C. Binet, J.C. Lawalley, G. Blanchard Catal. Today, 52 (1999), p. 53

[2] A. Tovarelli Catal. Rev. – Sci. Eng., 38 (1996), p. 439

[3] S. Tsunekawa, T. Fkuda, A. Kasuya J. Appl. Phys., 87 (2000), p. 1318

[4] M. Jiang, N.D. Wood, R. Komanduri J. Eng. Mater. Technol.: Trans. ASME, 120 (1998), p. 304

[5] H. Yahiro, Y. Baba, K. Eguchi, H. Arai J. Electrochem. Soc., 135 (1988), p. 2077

[6] F. Larachi, J. Pierre, A. Adnot, A. Bernis Appl. Surf. Sci., 195 (2002), p. 236

[7] R. DiMonte, P. Fornasiero, M. Graziani, J. Kašpar J. Alloys Compd., 277 (1998), p. 877

[8] M. Aresta, A. Dibenedetto, C. Pastore, A. Agelini, B. Aresta, I. Pápai J. Catal., 269 (2010), p. 44

[9] Ch.H. Wang, S.S. Lin Appl. Catal. A: Gen., 268 (2004), p. 227

[10] G. Bonura, F. Arena, G. Mezzatesta, C. Cannilla, L. Spadaro, F. Frusteri Catal. Today, 171 (2011) (251./.)

[11] X. Song, N. Jiang, Y. Li, D. Xu, G. Qui Mater. Chem. Phys., 110 (2008), p. 128

[12] R. Craciun Catal. Lett., 55 (1998), p. 25

[13] J. Strunk, W.C. Vining, A.T. Bell J. Phys. Chem. C, 115 (2011), p. 4114

[14] J. Sanchez-Valente, X. Bokhimi, J.A. Toledo Appl. Catal. A: Gen., 264 (2004), p. 175

[15] L. Katta, P. Sudarsnam, B. Mallesham, B.M. Reddy Catal. Sci. Technol., 2 (2012), p. 995

[16] U. Diebold Surf. Sci. Rep., 48 (2003), p. 53

[17] P.O. Larsson, A. Andersson J. Catal., 179 (1998), p. 72

[18] X. Jiang, L. Lou, Y. Chen, Z. Xiaoming Catal. Lett., 94 (2004), p. 49

[19] M. Berridge, D. Comar, C. Crouzel J. Appl. Radiat. Isot., 34 (1983), p. 1657

[20] E. Leino, P. Mäki-Arvela, V. Eta, D. Yu Murzin, T. Salmi, J.-P. Mikkola Appl. Catal. A: Gen., 383 (2010), p. 1

[21] I.E. Muskat, F. Strain, US Patent 2379250, 1941.

[22] H.P. Luo, W.D. Xiao Chem. Eng. Sci., 56 (2001), p. 4030

[23] B.C. Dunn, C. Guenneau, S.A. Hilton, J. Pahnke, E.M. Eyring, J. Dworzanski, H.L.C. Meuzelaar, J.Z. Hu, M.S. Solum, P. Pugmire J. Energy Fuel, 16 (2002), p. 177

[24] J.X. Zhen, S.Y. Hua, Ch.S. Hua Catal. Lett., 69 (2000), p. 153

[25] D. Wang, B. Yang, X. Zhai, L. Zhou Fuel Process. Technol., 88 (2007), p. 807

[26] C. Hao, S. Wang, X. Ma J. Mol. Catal. A: Chem., 306 (2009), p. 130

[27] E. Leino, P. Mäki-Arvela, K. Eränen, M. Tenho, D. Yu. Murzin, T. Salmi, J.-P. Mikkola Chem. Eng. J., 176-177 (2011), p. 124

[28] M. Honda, S. Kuno, N. Begum, K. Fujimoto, K. Suzuki, Y. Nakagawa, K. Tomishige Appl. Catal. A: Gen., 384 (2010), p. 165

[29] A. Dibenedetto, M. Aresta, A. Angelini, J. Ethiraj, B.M. Aresta Chem. Eur. J., 18 (2012), p. 10324

[30] M. Honda, S. Kuno, S. Sonehara, K. Fujimoto, K. Suzuki, Y. Nakagawa, K. Tomishige ChemCatChem, 3 (2011), p. 365

[31] M. Honda, M. Tamura, Y. Nakagawa, S. Sonehara, K. Suzuki, K. Fujimoto, K. Tomishige ChemSusChem, 6 (2013), p. 1341

[32] Y. Yoshida, Y. Arai, S. Kado, K. Kunimori, K. Tomishige Catal. Today, 115 (2006), p. 95

[33] W. Wang, S. Wang, X. Ma, J. Gong Catal. Today, 148 (2009), p. 323

[34] L. Wang, H. Li, S. Xin, P. He, Y. Cao, F. Li, X. Hou Appl. Catal. A: Gen., 471 (2014), p. 19

[35] The Rietveld Method. IUCr R.A. Young (Ed.), Oxford University Press, Oxford, UK (1993)

[36] D. Sherwood, B. Emmanuel Cryst. Growth Des., 6 (2006), p. 1415

[37] A.M. Garrido Pedrosa, M.J.B. Souza, D.M.A. Melo, A.S. Araujo, L.B. Zinner, J.D.G. Fernandes, A.E. Martinelli Solid State Sci., 5 (2003), p. 725

[38] Powder diffraction File 2 (PDF-2), sets 1–46, 1996 release, International Centre for Diffraction Data (ICDD).

[39] Inorganic Crystal Structure Database (ICSD), version 2.2., http://www.fiz-karlsruhe.de.icsd.html, 2013 Fiz Karlsruhe.

[40] J. Lee, S. Lee, E.A. Lee, H.J. Hwang Eco-Matter. Process. Des. Vii, 510–511 (2006), p. 1118

[41] Q. Yu, X. Wu, X. Yao, B. Liu, F. Goa, J. Wang, L. Dong Catal. Commun., 12 (2011), p. 1311

[42] K.M.S. Khalil J. Colloid Interface Sci., 307 (2007), p. 172

[43] Z.M. El-Bahy Mod. Res. Catal., 2 (2013), p. 136

[44] K. Bourikas, Ch. Kordulis, A. Lycourghiotis Chem. Rev., 114 (2013), p. 9754

[45] N. Wetchakum, B. Incessungvorn, K. Wetchakun, S. Phanichphant Mater. Lett., 82 (2012), p. 195

[46] P. Burroughs, A. Hamnett, A.F. Orchard, G. Thornton J. Chem. Soc. Dalton Trans., 17 (1976), p. 1686

[47] E. Beche, P. Charvin, D. Perarnau, S. Abanades, G. Flamant Short Commun., 40 (2008), p. 264

[48] S. Watanabe, X. Ma, Ch. Song J. Phys. Chem. C, 113 (2009), p. 14249

[49] S. Damyanova, J.M.C. Bueno Appl. Catal. A, 253 (2003), p. 135

[50] B.M. Reddy, B. Chowdhury, E.P. Reddy, A. Fernández Appl. Catal. A: Gen., 213 (2001), p. 279

[51] M. Francisco, P. Nascente, V. Mastelaro, A. Florentino J. Vac. Sci. Technol., 19 (2001), p. 1150

[52] L. Lu, S.L. Bernasek, J. Schwartz Surf. Sci., 458 (2000), p. 80

[53] C. Murugan, H.C. Bajaj Ind. J. Chem., 52A (2013), p. 459

[54] R. Srivastava, D. Srinivas, P. Ratnasamy J. Catal., 241 (2006), p. 34

[55] N. Kumar, E. Leino, P. Mäki-Arvela, A. Aho, M. Käldström, M. Tuominen, P. Laukkanen, K. Eränen, J.-P. Mikkola, D. Murzin Yu Micropor. Mesopor. Mater., 152 (2012), p. 71

[56] S. Damyanova, C.A. Perez, M. Schmal, J.M.C. Bueano Appl. Catal. A: Gen., 234 (2002), p. 271

[57] J. Goa, J. Guo, D. Liang, Z. Hou, J. Fei Int. J. Hydrogen Energy, 33 (2008), p. 5493

[58] A. Zhang, Z. Zhang, J. Chen, W. Sheng, L. Sun, J. Xiang Fuel Process. Technol., 135 (2015), p. 25

[59] Y.H. Taufiq-Yap, U. Rashid, Z. Zainal Appl. Catal. A: Gen., 468 (2013), p. 359 ArticleDownload PDFView Record in Scopus

[60] E. Leino, N. Kumar, P. Mäki-Arvela, A. Aho, K. Kordás, A.R. Leino, A. Shchukarev, D. Yu Murzin, J.P. Mikkola Mater. Chem. Phys., 143 (2013), p. 65

[61] B. M: Reddy, A. Khan, Y. Yamada, T. Kobayashi, S. Loridant, J.C. Volta J. Phys. Chem. B, 106 (2002), p. 10964

Tables and figures

Table 1. CO_2 uptake and specific surface area of ceria-supported catalysts.

Catalyst	**Basic sites (mmol/g)**				**Specific surface area (m^2/g)**	**Crystal size (nm)**
	Weak (320 K–500 K)	**Medium (500 K–750 K)**	**Strong (>750 K)**	**Total basicity**		
SiO_2 pristine	0.2	0.1	0.4	0.7	389	Amorphous
16 wt% CeO_2-SiO_2 evimp.	0.8	0.7	1.4	2.9	325	13.2[a]
16 wt% CeO_2-SiO_2 dp.	0.8	0.7	1.3	2.8	196	n.d.
γ-Al_2O_3 pristine	3.0	1.7	4.9	9.6	220	4.1
16 wt% CeO_2-Al_2O_3 evimp.	3.2	2.5	6.2	11.9	193	12.5[a]
16 wt% CeO_2-Al_2O_3 dp.	2.9	1.9	6.5	11.3	195	n.d.
TiO_2 pristine	0.1	0.5	0.1	0.7	200	19.4
16 wt% CeO_2-TiO_2 evimp.	0.4	0.8	0.8	2.0	29	10.8[a]
16 wt% CeO_2-TiO_2 dp.	0.5	0.8	0.9	2.2	31	n. d.
[a] crystallite size of CeO_2.						

Table 2. Specific surface area, average crystal size and total amount of basic sites of ceria-silica materials with varied CeO_2 loading.

Catalyst	**Average crystal size (nm)**	**Specific surface area (m^2/g)**	**Total basicity (mmol/g)**
8 wt% CeO_2-SiO_2	10.0	350	2.6
16 wt% CeO_2-SiO_2	13.2	325	2.9
32 wt% CeO_2-SiO_2	12.2	211	2.2

Table 3. Specific surface area and amount of basic sites of 16 wt% ceria-silica materials calcined at different catalysts.

Catalyst	Specific surface area (m^2/g)	Basic sites (mmol/g)			
		Weak	Medium	Strong	Total basicity
SiO_2 pristine	389	0.2	0.1	0.4	0.7
CeO_2-SiO_2-400 °C	340	0.3	0.3	1.6	2.2
CeO_2-SiO_2-600 °C	325	0.8	0.7	1.4	2.9
CeO_2-SiO_2-800 °C	192	0.2	0.1	0.1	0.4

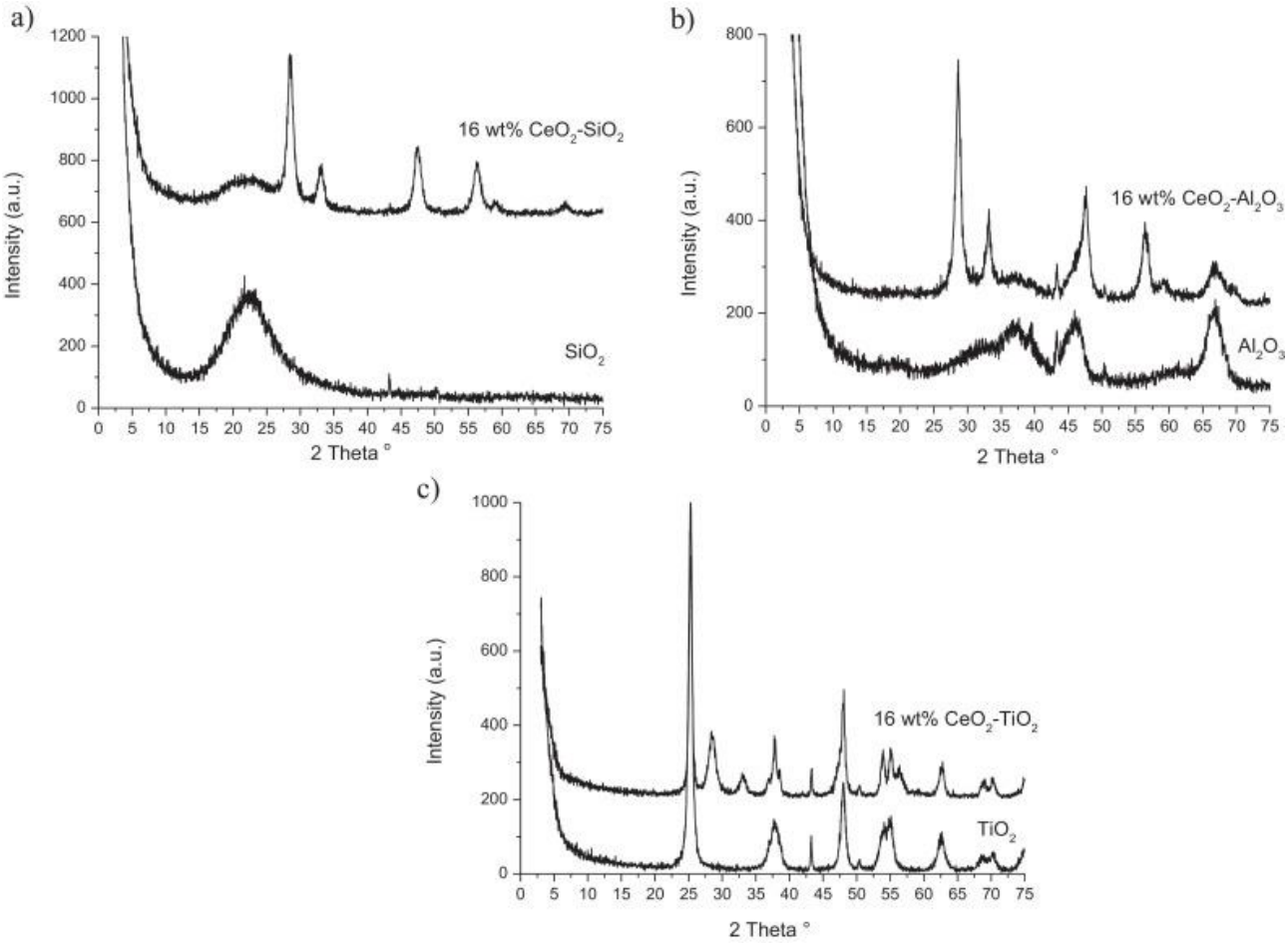

Fig. 1. X-ray diffraction patterns of the support and ceria-supported on (a) SiO_2; (b) Al_2O_3; (c) TiO_2 materials prepared via evaporation-impregnation method.

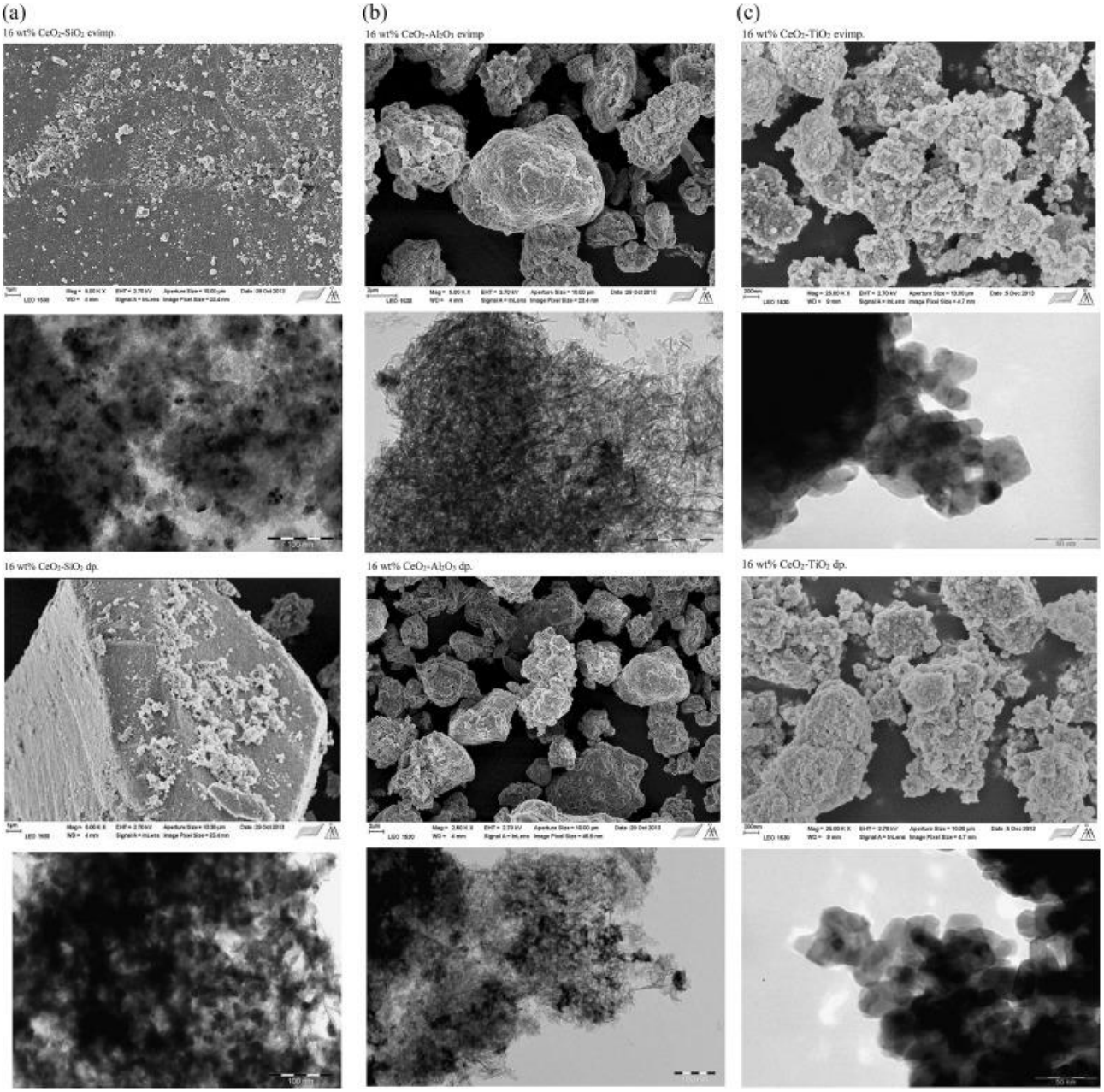

Fig. 2. SEM and TEM images of (a) ceria-supported on SiO_2, (b) ceria-supported on Al_2O_3 and (c) ceria-supported on TiO_2 materials synthesised by evaporation-impregnation (evimp.) and deposition-precipitation (dp.) method.

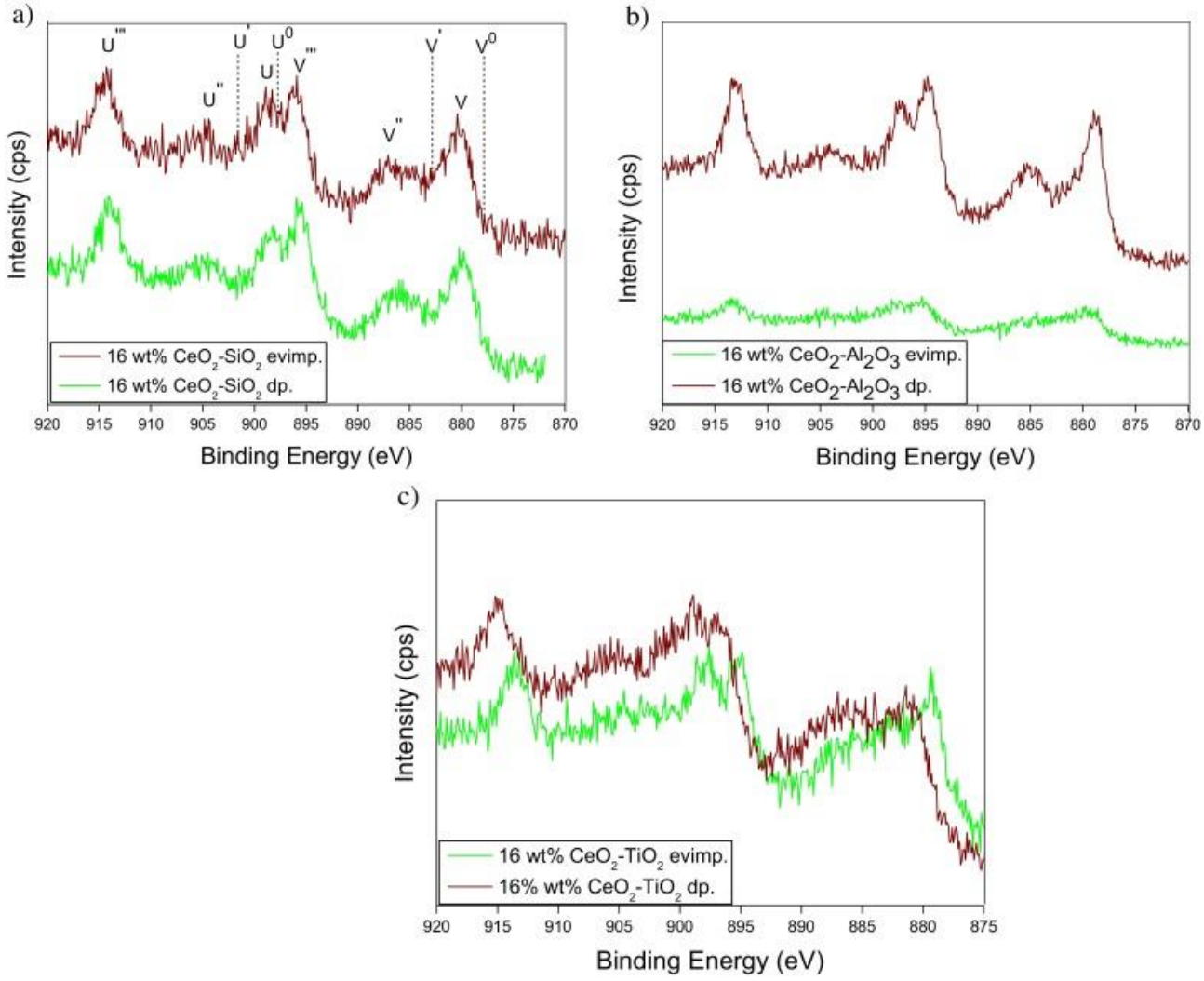

Fig. 3. XPS analysis spectra (a) ceria-supported on SiO_2, (b) ceria-supported on Al_2O_3 and (c) ceria-supported on TiO_2 materials prepared via evaporation-impregnation and deposition-precipitation method.

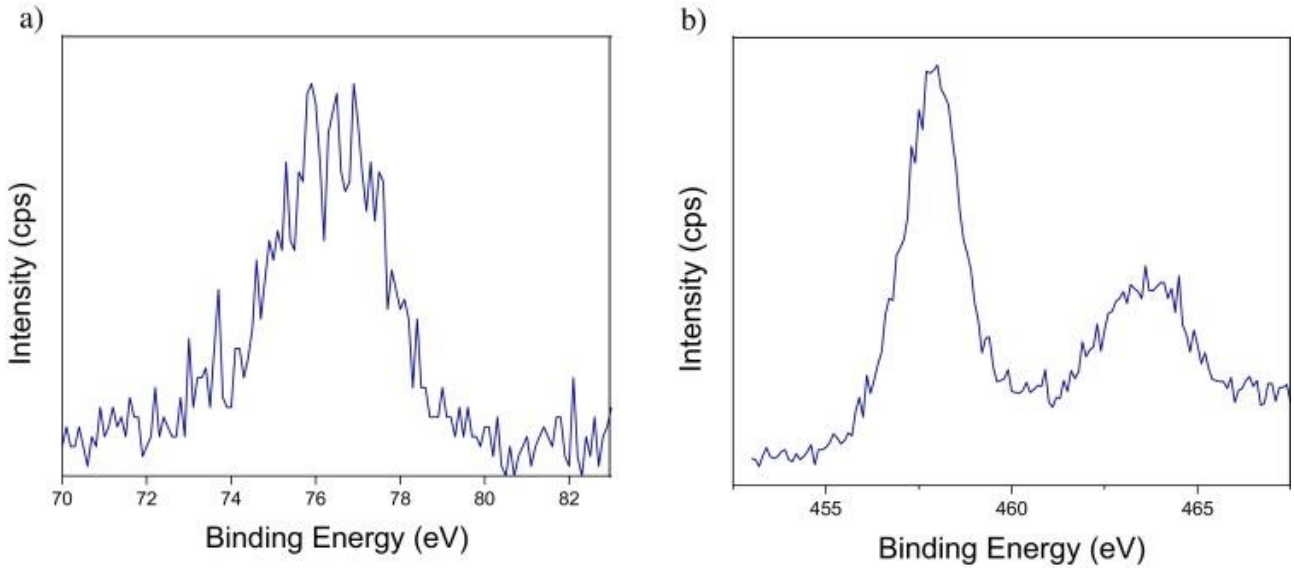

Fig. 4. XPS spectra of (a) Al 2p and (b) Ti 2p in 16 wt% CeO_2-Al_2O_3 and 16 wt% CeO_2-TiO_2 samples, respectively prepared by evaporation-impregnation method.

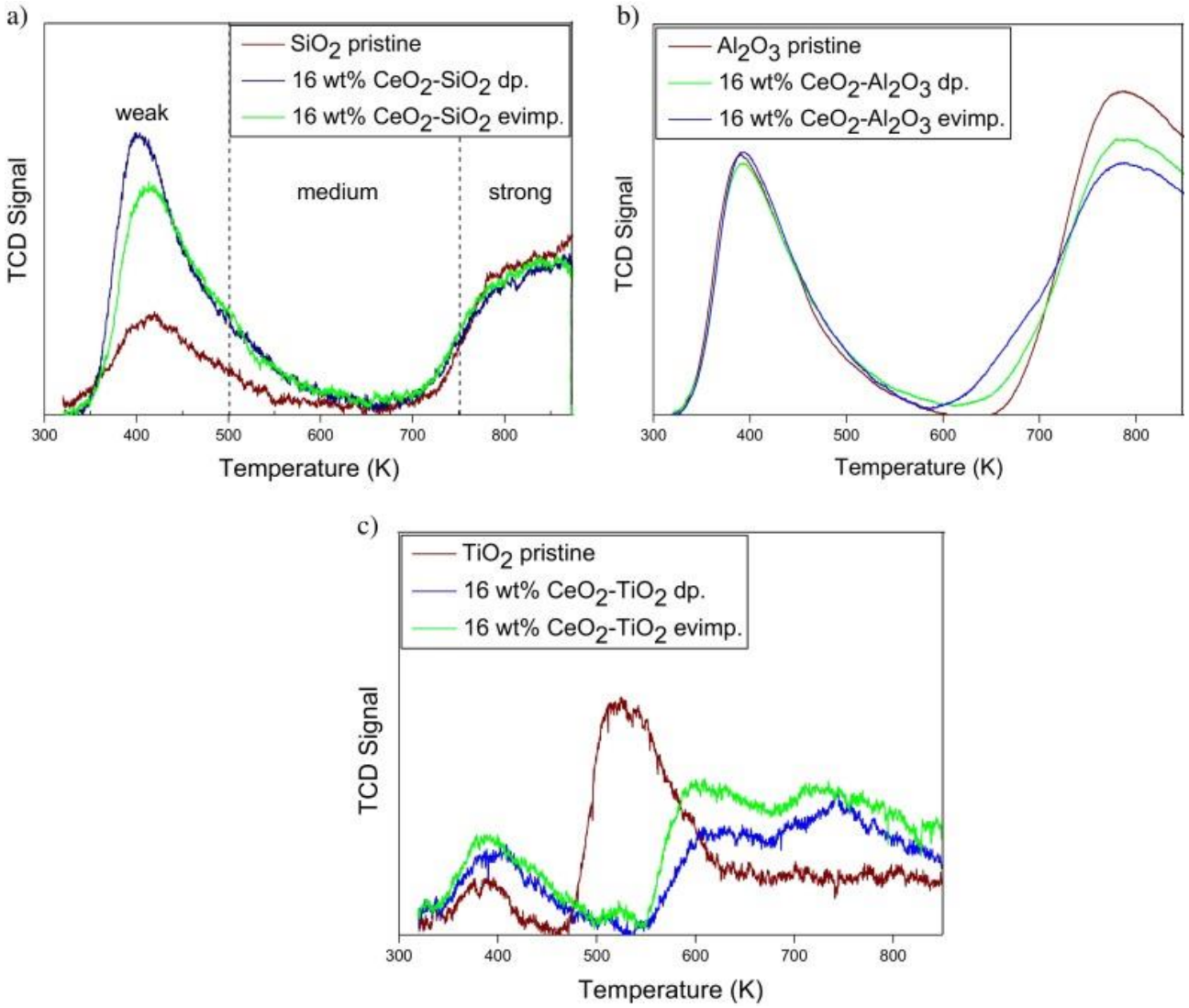

Fig. 5. CO_2-TPD profiles of ceria-supported on (a) SiO_2; (b) Al_2O_3; (c) TiO_2 materials prepared via evaporation-impregnation and deposition-precipitation method.

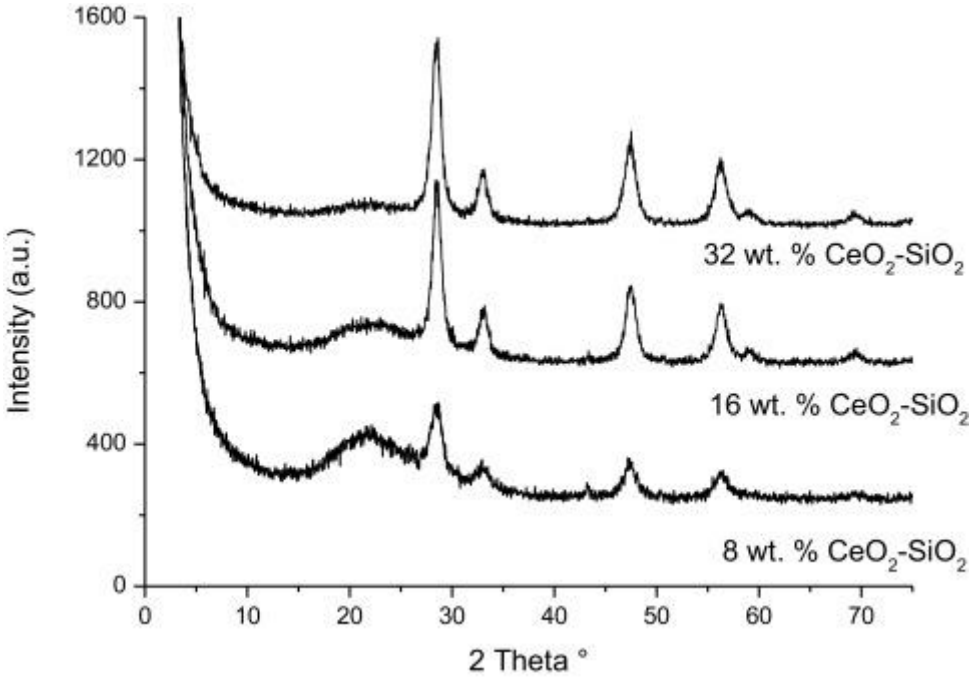

Fig. 6. X-ray diffraction patterns of CeO_2-SiO_2 samples with varied ceria loading.

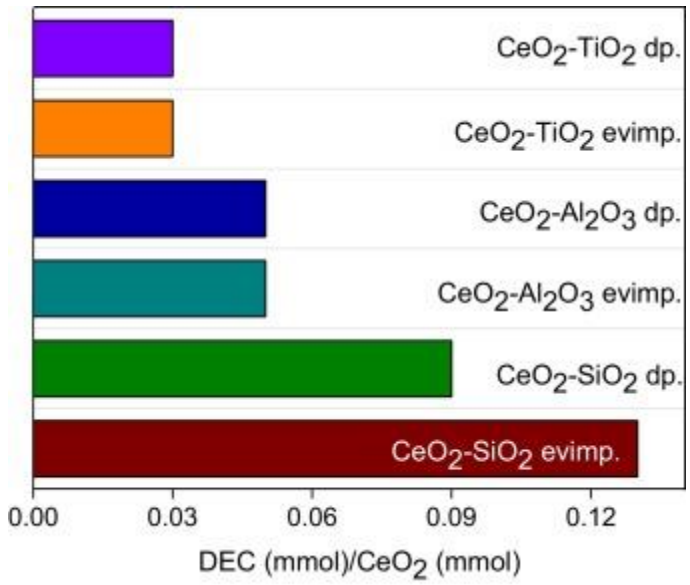

Fig. 7. Diethyl carbonate yield over 16 wt% CeO_2 supported on TiO_2, SiO_2 and Al_2O_3 catalysts prepared using evaporation impregnation (evimp.) and deposition precipitation (dp.). Conditions 1 g catalyst, 4.5 MPa initial CO_2 pressure, 314 mmol ethanol, 19 mmol butylene oxide, 25 h, 180 °C, ca. 700 rpm.

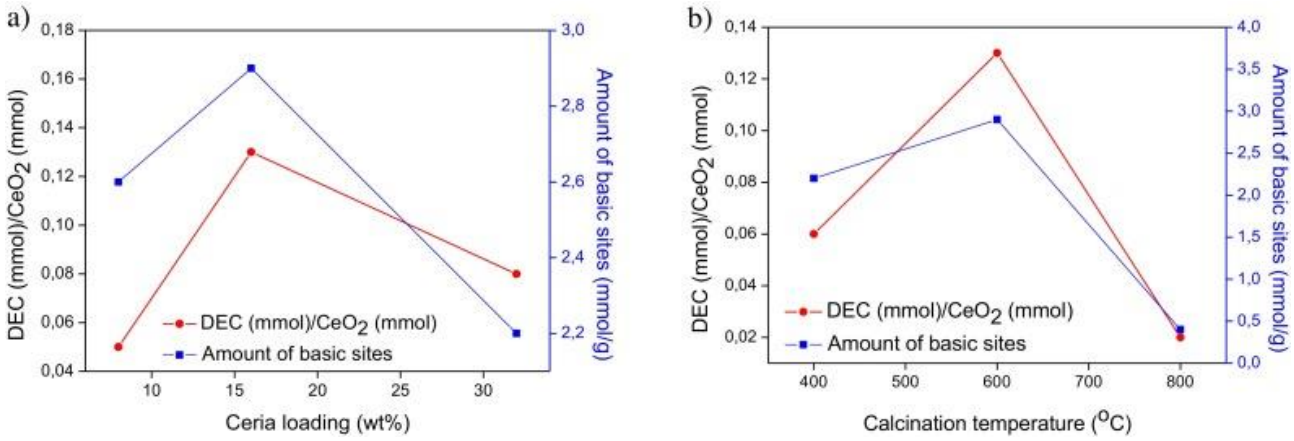

Fig. 8. Influence of CeO_2 loading and calcination temperature on the amount of basic sites and yield of diethyl carbonate. Conditions: 1 g catalyst, 4.5 MPa initial CO_2 pressure, 314 mmol ethanol, 19 mmol butylene oxide, 25 h, 180 °C, ca. 700 rpm.